Green Chemistry

Accepted Manuscript

ROYAL SOCIETY OF CHEMISTRY

www.rsc.org/greenchem

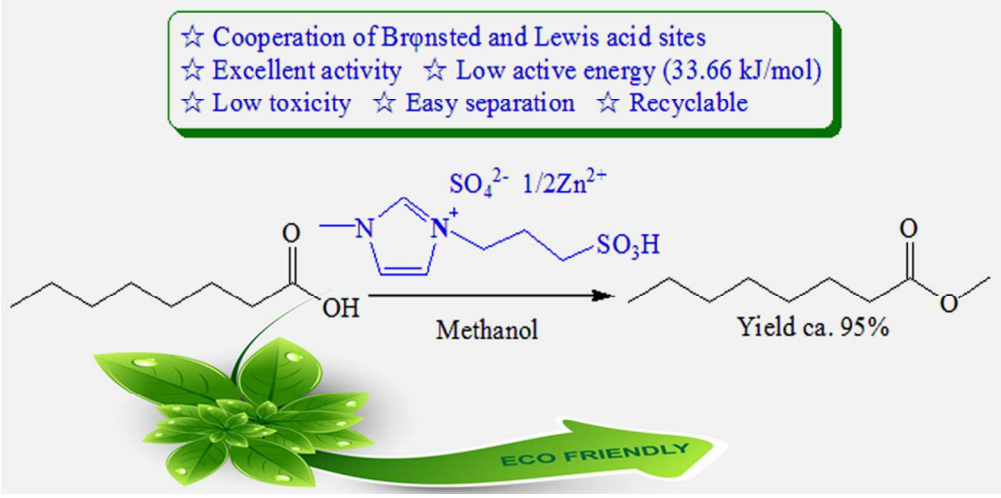

Cite this: DOI: 10.1039/c0xx00000x

www.rsc.org/greenchem

ARTICLE TYPE

Syntheses of novel halogen-free Brønsted-Lewis acidic ionic liquid catalysts and their applications for synthesis of methyl caprylate

Xiao-Xiang Han,[*,a] Huan Du,[a] Chin-Te Hung,[b] Li-Li Liu,[b] Pei-Hao Wu,[b] Da-Hai Ren,[c] Shing-Jong Huang[d] and Shang-Bin Liu[*,b,e]

Received (in XXX, XXX) Xth XXXXXXXXX 20XX, Accepted Xth XXXXXXXXX 20XX
DOI: 10.1039/b000000x

A series of benign halogen-free ionic liquid (IL) catalysts were synthesized by combining the Brønsted acidic ionic liquid $[HSO_3\text{-pmim}]^+HSO_4^-$ with ZnO in different composition ratios. The IL catalysts, which possess both Brønsted and Lewis acidity, were employed as acidic catalysts for esterification of *n*-caprylic acid to methyl caprylate. The $[HSO_3\text{-pmim}]^+(½Zn^{2+})SO_4^{2-}$, prepared by cooperating equimolar amount of Brønsted and Lewis acid sites, was found to exhibit an optimal catalytic performance and excellent durability. This is attributed to a synergy of Brønsted and Lewis acidity manifested by the catalyst. The response surface methodology (RSM) based on the Box-Behnken design (BBD) was utilized to explore the effects of different experimental variables (*viz.* catalyst amount, methanol to caprylic acid molar ratio, temperature, and reaction time) on esterification reaction. Analysis of variance (ANOVA) was also employed to study interactions between variables and their effects on the catalytic process. Accordingly, the deduced optimal reaction conditions led to a high methyl caprylate yield of 95.4%, in good agreement with experimental results and that predicted by the BBD model. Moreover, a kinetic study performed under optimal reaction conditions revealed an apparent reaction order of 1.70 and active energy of 33.66 kJ/mol.

Introduction

Esterification of alcohols and carboxylic acids are fundamental and important reactions in organic synthesis. The corresponding products, carboxylic esters, have been extensively applied in areas such as cosmetics, plastics, food, medicine and intermediates.[1] Conventionally, syntheses of carboxylic esters mostly invoke homogeneous catalysts, such as sulfuric, *p*-toluene sulfonic, and phosphoric acids. However, problems caused by these catalysts are not in conformity with the requirements of sustainable development, *e.g.*, equipment corrosion, environmental pollution, undesirable side reactions, plaguy catalyst recovery and reuse. To avoid these drawbacks, heterogeneous catalysts such as solid super acids,[2-5] heteropolyacid acids,[6] zeolites,[7-9] resins[10] and enzymes[11-14] have been employed for esterification. Unfortunately, limited applications were found for these solid catalysts due to the disadvantages such as low activity, easy deactivation, formidable separation and recovery and so on.[15] Hence, it is essential to develop environmental benign catalysts to replace the aforementioned catalysts.

Ionic liquids (ILs), which have been considered as new eco-friendly catalysts, have received considerable attention in various chemical syntheses owing to their unique characteristics such as low melting point, high thermal stability, negligible volatility, easy solubility, adjustable properties, recyclability, and reusability.[16, 17] Acidic ILs may be classified into Brønsted[18-28] and Lewis types[29,30] in accordance with their acidic groups. While various Brønsted-Lewis acidic ILs (B-L AILs) have been extensively developed and applied,[31,32] the most common types, which invoke incorporation of metal halides, are moisture-sensitive and hence are inapplicable for aqueous systems. To overcome this problem, efforts have been made in preparing halogen-free B-L AILs using copper oxide as the source of Lewis acidity.[33] Herein, we report a series of novel halogen-free B-L AIL catalysts synthesized by combining Brønsted acidic IL $[HSO_3\text{-pmim}]^+HSO_4^-$ with varied amount of ZnO as precursor for Lewis acidity. The acid catalysts so fabricated were characterized by a variety of different analytical and spectroscopic techniques, such as thermogravimetric analysis (TGA), Fourier transform infrared (FT-IR), and ^1H and ^{13}C nuclear magnetic resonance (NMR) spectroscopy. Moreover, the acidic properties of these B-L AILs were investigated by solid-state ^{31}P magic-angle spinning (MAS) NMR of adsorbed trimethylphosphine oxide (TMPO) as the probe molecule.[34-36] The catalytic activities of these B-L AILs during esterification of caprylic acid with methanol were investigated and relevant reaction conditions invoked during the synthesis of methyl caprylate were optimized using the response

[a] *Department of Applied Chemistry, Zhejiang Gongshang University, Hangzhou, 310035, China. Tel: +86-571-28008975; E-mail: hxx74@126.com*
[b] *Institute of Atomic and Molecular Sciences, Academic Sinica, Taipei 10617, Taiwan. Tel: +886-2-23668230; E-mail: sbliu@sinica.edu.tw*
[c] *Department of Chemical & Biomolecular Engineering, Clarkson University, Potsdam, New York 13699-5705, USA*
[d] *Instrumentation Center, National Taiwan University, Taipei 10617, Taiwan*
[e] *Department of Chemistry, National Taiwan Normal University, Taipei 11677, Taiwan*

surface methodology (RSM). The effects and correlations of different experimental variables such as catalyst amount, methanol to caprylic acid molar ratio, temperature, and reaction time on the esterification reaction were addressed by the Box-Behnken design (BBD) model, followed by a kinetic study performed under these optimized experimental parameters.

Experimental

Catalyst preparation

The novel B-L AIL catalysts were synthesized by combining sulfonic acid-functionalized Brønsted acidic ionic liquid $[HSO_3\text{-pmim}]^+HSO_4^-$ (denoted as ILa) with zinc oxide (ZnO). This was carried out by first preparing the $[HSO_3\text{-pmim}]^+HSO_4^-$ using a known procedure outlined in the literature,[37,38] followed by adding varied amounts of ZnO into the aqueous solution. The mixture was stirred continuously till the solid was completely dissolved. The resultant products were evacuated after water removal to obtain the final B-L AIL catalysts with varied L/B ratios, namely $[HSO_3\text{-pmim}]^+(½H^+·¼Zn^{2+})SO_4^{2-}$, $[HSO_3\text{-pmim}]^+(½Zn^{2+})SO_4^{2-}$, $[(½H^+·¼Zn^{2+})\ SO_3\text{-pmim}]^+\ (½Zn^{2+})SO_4^{2-}$, $[(½Zn^{2+})SO_3\text{-pmim}]^+(½Zn^{2+})SO_4^{2-}$, denoted as ILb, ILc, ILd, and ILe, respectively, as specified in Table 1.

Table 1 Characteristics of various acidic IL catalyst and their catalytic performances during esterification of caprylic acid with methanol

Catalyst			Conv.	Yield
Name	Formula	L/B[a]	(%)[b]	(%)[c]
ILa	$[HSO_3\text{-pmim}]^+HSO_4^-$	0:4	92.0	91.4
ILb	$[HSO_3\text{-pmim}]^+(½H^+·¼Zn^{2+})SO_4^{2-}$	1:3	93.0	92.5
ILc	$[HSO_3\text{-pmim}]^+(½Zn^{2+})SO_4^{2-}$	2:2	94.8	94.3
ILd	$[(½H^+·¼Zn^{2+})\ SO_3\text{-pmim}]^+\ (½Zn^{2+})SO_4^{2-}$	3:1	86.7	86.1
ILe	$[(½Zn^{2+})SO_3\text{-pmim}]^+(½Zn^{2+})SO_4^{2-}$	4:0	22.1	20.7
Null	---	---	5.3	4.8

[a] Molar ratio of Lewis/Brønsted acid sites.
[b] Reaction conditions: catalyst amount = 6 wt%, methanol/caprylic acid molar ratio = 5.0, reaction time = 3.0 h, and temperature = 363 K.
[c] Product yield of methyl caprylate determined by GC.

Catalyst characterization

FT-IR spectra of various AIL catalysts were obtained using KBr wafer conducted on a Bruker IFS-28 spectrometer in the region of 4000-400 cm^{-1}. All thermogravimetric and differential thermogravimetric (TG-DTG) curves were recorded on a TG-209 (NETZSCH) thermal analyzer. Samples were heated from room temperature (RT; 298 K) to 873 K at a heating rate of 10 K/min under dynamic N_2 atmosphere. ^1H and ^{13}C NMR spectra were acquired on a Bruker AV-500 spectrometer.[37,38] Solid-state ^{31}P MAS NMR measurements were performed on a Bruker-Biospin Avance-III 500 spectrometer at a Larmor frequency of 202.46 MHz using a 4-mm double-resonance MAS probehead. ^{31}P spectra were acquired using a single-pulse sequence under a sample spinning rate of 12 kHz using an excitation pulse of 1.5 μs (π/6 pulse) and a recycle delay of 10 s. The ^{31}P chemical shifts were referenced to 85% H_3PO_4 aqueous solution.

Detailed acid features, namely types, relative concentration, and strength of Brønsted vs Lewis acidity in the B-L AIL catalysts were studied by ^{31}P MAS NMR of adsorbed TMPO.[34-36] Prior to the adsorption of TMPO probe molecule, each catalyst was first subjected to dehydration treatment at 393 K for 24 h under vacuum (< 10^{-5} Torr). Subsequently, a known amount of TMPO dissolved in anhydrous CH_2Cl_2 was introduced into a vessel containing the dehydrated sample in a glove box under N_2 environment. The sealed sample vessel was then connected to a vacuum manifold, followed by removal of the CH_2Cl_2 solvent by evacuation at 323 K. Furthermore, the sample was subjected to thermal treatment at 393 K for at least 24 h to ensure a uniform adsorption of adsorbate probe molecules in the substrate. Finally, the TMPO-loaded sample was transferred into a MAS rotor in a N_2 glove box and then sealed by a gas-tight Kel-F cap.

Esterification reaction

n-Caprylic acid (0.1 mol), a desirable amount of methanol, and a known amount of the AIL catalyst were placed into a three-necked flask equipped with a mechanical stirrer, reflux condenser, and a drop funnel containing microporous 3A molecular sieves to absorb water produced from esterification. The esterification of *n*-caprylic acid with methanol was first carried out at different temperatures for a desired period of time, then, the reaction mixture was cooled to RT. Typically, owing to the self-separation characteristics of the reaction system, the reaction mixture tends to spontaneously separate into two layers. The upper layer was extracted by distillation to obtain the methyl caprylate product, and the lower layer consisting of AIL catalyst was reused after further treatment. Quantitative analysis of the products was performed by gas chromatography using an Agilent 6890N GC apparatus equipped with a FID detector and HP-5 capillary column. Reactants and products were identified by comparison with authentic samples using methyl laurate as an internal standard.

The conversion of *n*-caprylic acid was calculated as follows:

$$\text{Conversion} = (1 - a_1 / a_2) \times 100\%, \quad (1)$$

where a_1 and a_2 represents the initial and final acidity of the reaction mixture, respectively. The acidity values were monitored by sodium hydroxide (NaOH) titration.

Design of experiments and response surface methodology

Response surface methodology (RSM)[39,40] was employed to obtain optimal experimental conditions for esterification of caprylic acid with methanol. A Box-Behnken design (BBD) was applied to study the effects of three process variables, namely amount of catalyst (x_1), methanol to caprylic acid molar ratio (x_2), and reaction time (x_3), as specified in Table 2. A total of 17 experimental sets, which included 12 factorial points and 5 centring points, were adopted. The three experimental variables were designed at three levels coded with a plus signs (+1; high value), zero (0; central value), or a minus signs (-1; low value). The coded values of these factors were obtained by the equation:

$$x_i = \frac{X_i - X_0}{\Delta X_i} \quad (2)$$

where x_i, X_i, and X_0 (i = 1–3) represents the coded, real, and central value of the independent variable, respectively, and ΔX_i = (variable at high level − variable at low level)/2, which denotes the step change value.

Table 2 List of symbols and coded levels for corresponding experimental variables and ranges adopted for the esterification process*

Variable (unit)	Symbol	Range and level		
		-1	0	1
Catalyst amount (wt%)	x_1	4.0	6.0	8.0
Methanol/caprylic acid ratio (mol/mol)	x_2	2.5	5.0	7.5
Reaction time (h)	x_3	1.5	2.0	2.5

*Over the $[HSO_3\text{-pmim}]^+(½Zn^{2+})SO_4^{2-}$ catalyst at 363 K.

A model equation based on quadratic polynomial given by RSM was used to reveal interactive effects between experimental variables, to optimize the reaction process, and to predict the yield of the product (i.e., methyl caprylate). The model equation may be expressed as:

$$Y = \beta_0 + \sum_{i=1}^{3} \beta_i x_i + \sum_{i=1}^{3} \beta_{ii} {x_i}^2 + \sum_{i<j}^{3} \beta_{ij} x_i x_j \quad (3)$$

where Y is the predicted response (i.e., product yield), x_i and x_j are the coded levels of the independent variables, β_0, β_i, β_{ii}, and β_{ij} denote the regression coefficient representing the offset, linear, quadratic, and interaction term, respectively. A Design-Expert 6.0.5 software (Stat-Ease, USA) was used to analyse the experimental data, to perform analysis of variance (ANOVA), and to evaluate the regression equation. Accordingly, the fitted polynomial equation may further be expressed in terms of response surface and contour plots to facilitate visualization of the correlations between the response and experimental variables at various coded levels, and to infer optimized process conditions. The coefficient of determination (R^2) may be used to evaluate the accuracy and applicability of the second order multiple regression model. The significance of its regression coefficient was checked with the F-test value.

Kinetic study

The reaction rate (r) for esterification of n-caprylic acid to methyl caprylate may be expressed as:

$$r = -\frac{dC_A}{dt} = k_+ {C_A}^{\alpha} {C_B}^{\beta} - k_- {C_C}^{\gamma} {C_D}^{\eta} \quad (4)$$

where C_A, C_B, C_C, and C_D represent the instant concentration of n-caprylic acid, methanol, methyl caprylate, and water, respectively, while α, β, γ, and η denote their corresponding reaction order. Whereas, k_+ and k_- account for the rate constants associate with the forward and inverse reaction, respectively.

Given that water had been effectively removed by microporous 3A zeolite adsorbent during esterification reaction, the reaction could be considered as an irreversible process. In this context, the second term associated with inverse process in Eq. (4) may be ignored. Moreover, since the concentration of methanol is always much higher than that of n-caprylic acid, $k_+ {C_B}^{\beta}$ in Eq. (4) could be deemed as constant, leading to a simplified rate equation:

$$r = -\frac{dC_A}{dt} = k {C_A}^{\alpha} \quad (5)$$

where $k = k_+ {C_B}^{\beta}$ refers to the modified rate constant. By taking the natural logarithm, Eq. (5) may further be expressed as:

$$\ln r = \ln k + \alpha \ln C_A \quad (6)$$

The values of k and α at different temperatures may therefore be obtained easily by linear fitting of the ln r vs ln C_A curve using the Origin 8.5 software.

It is well-known that the variation of reaction rate with temperature may be expressed by the Arrhenius equation as:

$$\ln k = \ln k_0 - \frac{E_a}{R} \frac{1}{T} \quad (7)$$

Thus, the activation energy (E_a) and pre-exponential factor (k_0) may be derived from the slope and intercept of the Arrhenius (ln k vs 1/T) plot.

Results and discussion

Catalyst characterization

Similar ^{1}H and ^{13}C NMR spectra were observed for various B-L AIL catalysts. As an example, the NMR data obtained from $[HSO_3\text{-pmim}]^+(½Zn^{2+})SO_4^{2-}$ (i.e. ILc) catalyst having equimolar amount of Brønsted and Lewis acid sites are depicted below: ^{1}H NMR (500 MHz, D_2O): δ 2.31 (m, 2H), 2.91 (t, 2H), 3.89 (s, 3H), 4.36 (t, 2H), 7.44 (s, 1H), 7.51 (s, 1H), 8.74 (s, 1H) ppm; ^{13}C NMR (500 MHz, D_2O): δ 27.57, 38.20, 49.69, 50.21, 124.68, 126.26, 138.68 ppm.

Fig. 1 displays the FT-IR spectra of various IL catalysts specified in Table 1. In spite of the marginal variations in peak intensities and peak positions, distinct characteristic vibrational bands responsible for Brønsted acidic IL $[HSO_3\text{-pmim}]^+HSO_4^-$ were observed before (ILa) and after substitution of protons (H^+) with Zn^{2+} cations. The absorption peaks at 1638 and 1573 cm^{-1} may be attributed to the stretching vibrations of C=C and C=N bonds on the imidazole ring, respectively. The peak at 2930 cm^{-1} should be associated with asymmetric stretching vibration of $–CH_2$ and the bonds at 1460 and 748 cm^{-1} may be assigned to bending and rocking vibrations of $–CH_3$, respectively. Whereas the strong absorption bonds at 1080 and 1045 cm^{-1} may be attributed to the asymmetric and symmetric stretching vibrations of S=O, respectively. Moreover, a notable decrease in peak intensity of the band responsible for –OH vibration at 3400 cm^{-1} with increasing substitution of H^+ with Zn^{2+} ions (i.e., increasing L/B ratio in Table 1) was observed, revealing the progressive incorporation of Lewis acidity onto the pristine Brønsted acidic (ILa) catalyst.[41,42]

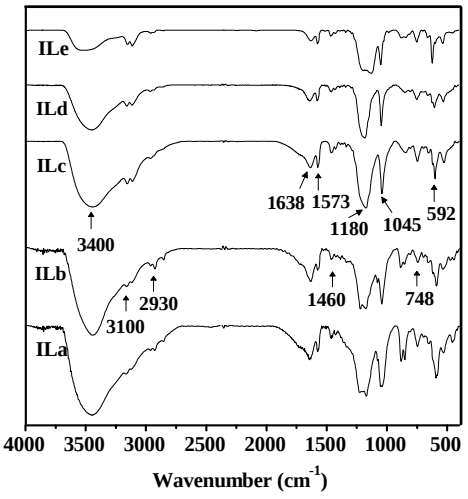

Fig. 1 FT-IR spectra of various IL catalysts: ILa = $[HSO_3\text{-pmim}]^+HSO_4^-$, ILb = $[HSO_3\text{-pmim}]^+(½H^+·¼Zn^{2+})SO_4^{2-}$, ILc = $[HSO_3\text{-pmim}]^+(½Zn^{2+})SO_4^{2-}$, ILd = $[(½H^+·¼Zn^{2+})\ SO_3\text{-pmim}]^+\ (½Zn^{2+})SO_4^{2-}$, and ILe = $[(½Zn^{2+})SO_3\text{-pmim}]^+(½Zn^{2+})SO_4^{2-}$.

TGA-DTG analyses were performed to investigate thermal stability of various AIL catalysts. Since similar TGA-DTG profiles were observed for most B-L AIL catalysts over the temperature range from RT to 873 K, only assorted TGA-DTG results obtained from the zwitterion 1-sulfonicacidpropyl-3-methylimidazole (MIMPS), Brønsted acidic ILa ([HSO_3-

pmim]$^{+}HSO_4^{-}$), and B-L AIL with L/B = 1.0 (i.e. ILc) samples are illustrated and discussed. The TGA curves observed for MIMPS and ILa showed similar weight-loss profiles at ca. 300–380 and 575-675 K. For the latter ILa ([HSO_3-pmim]$^{+}HSO_4^{-}$) catalyst, an initial weight loss occurred at 356 K (Fig. 2b), which may be attributed to desorption of physisorbed water, while the second weight-loss peak was observed at 625 K, corresponding to the decomposition of the organic MIMPS (Fig. 2a). By comparison, the TGA-DTG profile of [HSO_3-pmim]$^{+}$(½Zn^{2+})SO_4^{2-} (i.e., ILc) shown in Fig. 2c revealed two major weight-loss peaks at 333 and 636 K. Thus, the acidic ILc catalyst appeared to be thermally more stable than ILa after incorporating Lewis acidity. It is noteworthy that these novel B-L AILs (such as [HSO_3-pmim]$^{+}$(½Zn^{2+})SO_4^{2-}) retain their structural integrity over the range of reaction temperatures (323–363 K) examined.

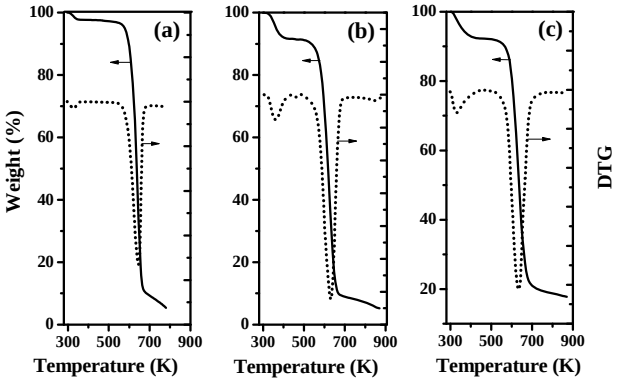

Fig. 2 TG-DTG curves of (a) MIMPS, (b) [HSO_3-pmim]$^{+}HSO_4^{-}$, and (c) [HSO_3-pmim]$^{+}$(½Zn^{2+})SO_4^{2-}.

Solid-state ^{31}P MAS NMR of adsorbed TMPO has been proven to be a feasible and powerful approach for characterization of acid properties of solid acid catalysts.[34-36,40,43] The base TMPO probe molecule tends to interact with the acidic proton to form $TMPOH^{+}$ complex. It has been demonstrated that a linear correlation between the observed ^{31}P NMR chemical shift (δ^{31}P) and acidic strength of Brønsted acidity may be inferred by means of such ^{31}P-TMPO NMR approach.[34-36] A higher observed δ^{31}P value of the adsorbed TMPO therefore represents stronger acidic strength of the catalyst, and *vice versa*. Fig. 3 shows ^{31}P NMR spectra of TMPO adsorbed on various AILs. The ^{31}P spectrum of ILa exhibited a sharp singlet at 86.2 ppm, indicating the sole presence of Brønsted acidity whose average strength is in the proximity of the threshold for superacidity (86 ppm).[34-36,40] It is indicative that the parent [HSO_3-pmim]$^{+}HSO_4^{-}$ catalyst indeed possesses ultra-strong Brønsted acidity. Upon progressing incorporation of Lewis metallic center (Zn^{2+}), the ^{31}P resonances become broaden due to consistent increase in viscosity. This is also accompanied by a gradual decrease in δ^{31}P. For examples, a single broad resonance peak was observed for TMPO adsorbed on ILb and ILc, corresponding to δ^{31}P of 81 and 77 ppm, respectively. Clearly, Brønsted acidity became weaker as more H^{+} are being substituted by the Zn^{2+} ion, creating Lewis acidity. On the other hand, multiple resonances were observed for ILd and Ile, among them, the peak in the vicinity of 63 ppm may be attributed to the presence of Lewis acidity.[34,35,43] Thus, we assign the two peaks observed for ILd at 77 and 66 ppm due to TMPO adsorbed on Brønsted and Lewis acid sites, respectively. In this context, the broad multiple resonance around 63 ppm in ILe indicates that the AIL mainly manifests Lewis acidity. In terms of viscosity of these AILs, ILa, ILb, and ILc were found to exhibit a liquid phase with increasing viscosity, but ILd appeared to be a mixture of liquid with solid, whereas ILe was a solid powder. These results are in line with the δ^{31}P and corresponding linewidths of the adsorbed TMPO in various catalyst substrates.

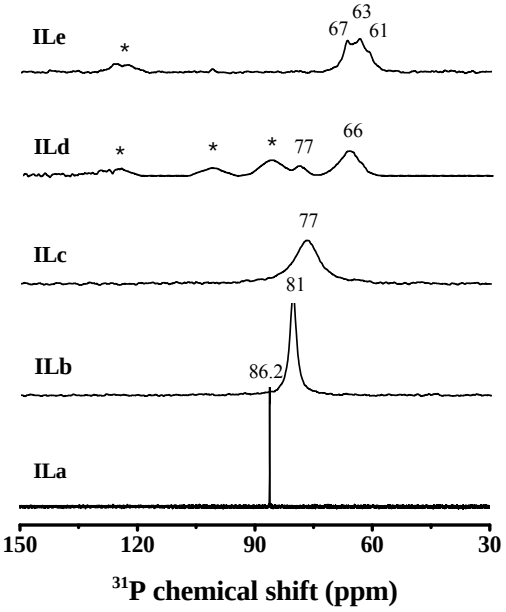

Fig. 3 ^{31}P NMR spectra of various acidic IL catalysts: ILa = [HSO_3-pmim]$^{+}HSO_4^{-}$, ILb = [HSO_3-pmim]$^{+}$(½H^{+}·¼Zn^{2+})SO_4^{2-}, ILc = [HSO_3-pmim]$^{+}$(½Zn^{2+})SO_4^{2-}, ILd = [(½H^{+}·¼Zn^{2+}) SO_3-pmim]$^{+}$ (½Zn^{2+})SO_4^{2-}, ILe = [(½Zn^{2+})SO_3-pmim]$^{+}$(½Zn^{2+})SO_4^{2-}. The asterisks in the spectra denote spinning sidebands.

Role of Brønsted and Lewis acidity on catalytic activity

To explore the effects and correlations of Lewis and Brønsted acid sites on catalytic performance during esterification of *n*-caprylic acid with methanol. Catalytic activities of various AIL catalysts were attained, as summarized in Table 1. Accordingly, it is indicative that Brønsted acid sites played the primary role than Lewis acidity during catalytic esterification reaction. This may be seen by the notable decreases in conversion and product yield with increasing Lewis acidity. Nevertheless, the ILa catalyst, which solely possesses ultra-strong Brønsted acidity, showed inferior catalytic activity compared to ILb and ILc. This reveals that ultra-strong acidity may be unfavorable for esterification reaction, likely due to the occurrence of acid-catalysed reverse reactions. Interestingly, optimal conversion (94.8%) and methyl caprylate yield (94.3%) were obtained when equimolar Lewis and Brønsted acid sites were incorporated in the AIL (i.e., ILc). On the basis of these results, it is indicative that a synergy of Lewis and Brønsted acid sites manifests the catalytic activity during formation of methyl caprylate over these novel AIL catalysts, particularly when an equimolar amount of both types of acidities was implemented. A possible catalytic mechanism is proposed in Scheme 1. In brief, the Lewis center (Zn^{2+}) may incorporate with

the oxygen atom in the carbonyl groups, which possess strong electronegativity, to induce interactions between the oxygen in the alcohol hydroxyl group and the carbon atom in the carbonyl group. On the other hand, couplings of Brønsted acidic H^+ with the oxygen atom in the carbonyl group tends to lower the negative charge, hence, is favorable for the release of Zn^{2+}.

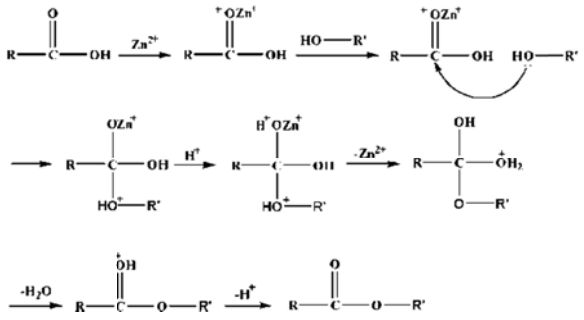

Scheme 1 Possible mechanism invoked during esterification of *n*-caprylic acid with methanol over the B-L AIL $[HSO_3\text{-pmim}]^+(½Zn^{2+})SO_4^{2-}$ catalyst.

Effects of experimental variables on esterification

Since the $[HSO_3\text{-pmim}]^+(½Zn^{2+})SO_4^{2-}$ AIL catalyst having the Lewis/Brønsted molar ratio of 1:1 exhibited the best catalytic performance, the ILc catalyst was chosen for further process optimization study. Four important experimental variables, namely the catalyst amount, methanol/*n*-caprylic acid reactant ratio, reaction time, and temperature, were investigated. Among them, the amount of catalyst used plays a key role during esterification due to its high effectiveness to the whole reaction process. Fig. 4a shows the effect of $[HSO_3\text{-pmim}]^+(½Zn^{2+})SO_4^{2-}$ loading on catalytic activity during esterification of *n*-caprylic acid with methanol. It is noteworthy that while performing the experiments with varied catalyst loading, other experimental parameters were kept constants: methanol/caprylic acid ratio = 5.0, reaction time = 3.0 h, and temperature = 363 K. Accordingly, a consistent increases in both conversion and methyl caprylate yield with increasing amount of catalyst dosage was observed, eventually reaching a respective plateau for conversion (94.8%) and product yield (94.3%) at a reaction time of 3 h and a catalyst loading of 6 wt%. This is likely due to the suitable amount of active moieties desirable for the reaction. However, as the catalyst amount exceeded 6 wt%, the conversion of *n*-caprylic acid and yield of methyl caprylate retained practically unchanged. This may be attributed to dissolution of the AIL catalyst in the presence of methanol, but the catalyst is practically unsolvable in methyl caprylate. As such, at a prolonged reaction time, as the product ester became the primary component of the reaction mixture, leading to the limited solubility of the catalyst. Thus, in view of the observed high yield of methyl caprylate and the relevant cost effectiveness issue of the process, an optimal catalyst amount of ca. 6 wt% may be inferred.

Regarding to the effect of feeds, Fig. 4b displays the variation of methanol to *n*-caprylic acid molar ratio on esterification activity. It was found that, as the reactant ratio increased, the initial yield of ester also increased significantly and eventually leveled off at 94.3% when the ratio of methanol to caprylic acid reached 5:1. Since esterification is a reversible reaction, an adequate amount of methanol is required to drive the equilibrium towards formation of methyl caprylate. Meanwhile, the AIL catalyst is highly soluble in methanol, thus, resulted in a homogeneous distribution of catalyst in the reaction mixture to provoke efficient esterification reaction. Nonetheless, as the ratio of methanol to caprylic acid exceeded 5:1, the excessive methanol no longer had decisive impact on the conversion rate and product yield due to dilution of the catalyst in the reaction mixture.

Influence of reaction time and temperature on the esterification was also investigated, as shown in Figs. 4c and 4d. It is evident that the methyl caprylate yield reached ca. 88.9% rapidly during the initial stage (1.0 h), then increased gradually till reaching a maximum of 94.4% at 2.0 h. A marginal decrease in product yield beyond reaction time of 2.0 h was observed, mostly likely due to partial hydrolization of methyl caprylate. As for effect of reaction temperature, the yield of methyl caprylate reached a maximum as the temperature reached 363 K at 2.0 h. However, while water removal by methanol evaporation may be more efficient at higher temperatures, no further increase in *n*-caprylic acid conversion and product yield was observed above 363 K, likely due to inevitable loss of methanol above its boiling point.

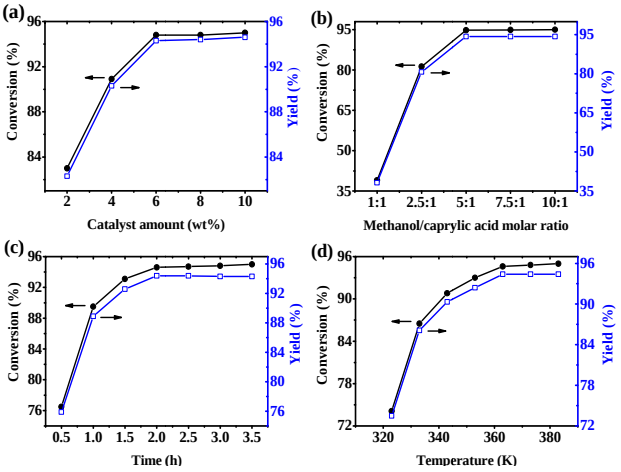

Fig. 4 Effects of (a) catalyst amount, (b) substrates molar ratio, (c) reaction time, and (d) temperature on conversion and methyl caprylate yield during esterification of *n*-caprylic acid with methanol over the $[HSO_3\text{-pmim}]^+(½Zn^{2+})SO_4^{2-}$ catalyst. Note that while varying each experimental variable, other parameters were kept constants at their predicted optimal values: catalyst amount = 6 wt%, methanol/caprylic acid molar ratio = 5.0, reaction time = 2–3 h, and temperature = 363 K.

Process and product optimization

The factorial experimental design was applied to minimize the waste of catalyst and to reduce the number of cumbersome experiments without significant loss of information. The design of experiments, experimental results, and predicted responses for the esterification of *n*-caprylic acid with methanol over the $[HSO_3\text{-pmim}]^+(½Zn^{2+})SO_4^{2-}$ catalyst are summarized in Table 3. No significant difference between experimental results and predicted data can be found. The methyl caprylate yield (Y) may be correlated with independent experimental variables by a quadratic model, which can be expressed as:

$$Y = +94.37 + 2.78x_1 + 8.80x_2 + 3.17x_3 - 2.97x_1^2 - 8.23x_2^2 - 1.88x_3^2 - 0.67x_1x_2 - 1.37x_1x_3 - 1.69x_2x_3 \quad (8)$$

where x_1, x_2 and x_3 are the coded values respectively representing three experimental variables, namely catalyst amount, molar ratio of alcohol to acid, and reaction time (*cf.* Table 2).

Table 3 List of experimental design and response values during esterification of *n*-caprylic acid with methanol over the $[HSO_3\text{-pmim}]^+(½Zn^{2+})SO_4^{2-}$ catalyst

Entry	Variable and level[a]			Methyl caprylate yield (%)	
	x_1	x_2	x_3	Experimental	Predicted
1	-1	-1	0	71.01	70.93
2	1	-1	0	77.18	77.82
3	-1	1	0	90.51	89.87
4	1	1	0	94.00	94.08
5	-1	0	-1	81.92	82.21
6	1	0	-1	90.93	90.50
7	-1	0	1	90.85	91.28
8	1	0	1	94.40	94.11
9	0	-1	-1	70.82	70.61
10	0	1	-1	91.24	91.59
11	0	-1	1	80.68	80.33
12	0	1	1	94.33	94.54
13	0	0	0	94.97	94.37
14	0	0	0	93.93	94.37
15	0	0	0	94.23	94.37
16	0	0	0	93.82	94.37
17	0	0	0	94.89	94.37

[a] Variables and levels specified in Table 2.

The fitting quality of the quadratic model (Eq. 8) was verified by the standard analysis of variance (ANOVA) presented in Table 4. The model *F*-value (309.76) was much greater than the tabular counterpart ($F_{0.01, 9, 7} = 6.71$), implied that the model was indeed significant. In addition, the obtained *P*-value (< 0.0001) revealed that the chance (0.01%) such a large 'model *F*-value' could occur was close to noise level. The observed "Lack of Fit *F*-value" of 2.00 also implied that the Lack of Fit was not significant relative to pure error. A coefficient of determination ($R^2 = 0.9975$ was attained, indicating that the model was reliable in predicting the response. The "Adeq Precision" (48.755), which measured the signal to noise ratio, was also much greater than the desirable value of 4, as expected. Moreover, the coefficient of variation (C.V. = 0.73%) also demonstrated that the experiments were carried out reliably. On the basis of these statistical values, it is conclusive that the quadratic model was adequate to predict a reliable methyl caprylate yield within the range of the variables studied. This is supported by the observed *F*- and *P*-values, which revealed that all three independent variables were highly significant, and that the order of their significance was methanol/caprylic acid molar ratio > reaction time > amount of catalyst to *n*-caprylic acid. Moreover, mutual interactions between each pair of these independent variables were also highly significant to the esterification reaction.

Table 4 Estimated regression coefficients and corresponding *F*- and *P*-values for methyl caprylate yield.

Source	Sum of squares	Degree of Freedom	Mean square	*F*-value	P-value	Significance
model	1142.19	9	126.91	309.76	< 0.0001	**
x_1	61.72	1	61.72	150.63	< 0.0001	**
x_2	619.34	1	619.34	1511.67	< 0.0001	**
x_3	80.33	1	80.33	196.06	< 0.0001	**
x_1^2	37.08	1	37.08	90.51	< 0.0001	**
x_2^2	284.86	1	284.86	695.28	< 0.0001	**
x_3^2	14.81	1	14.81	36.14	0.0005	**
$x_1 x_2$	1.80	1	1.80	4.38	0.0746	
x_1x_3	7.45	1	7.45	18.19	0.0037	**
x_2x_3	11.46	1	11.46	27.97	0.0011	**
Residual	2.87	7	0.41			
Lack of fit	1.72	3	0.57	2.00	0.2559	
Error	1.15	4	0.29			
Cor total	1145.06	16				

** represents highly significant.

The three dimensional (3-D) response surface and contour plots obtained from the predicted model are shown in Fig. 5. The correlations between methanol/*n*-caprylic acid molar ratio and catalyst amount at a fixed reaction temperature and time are shown in Figs. 5a and 5d. It is clear that the yield of methyl caprylate rapidly increased to the optimal value with increasing methanol/acid molar ratio, however, no much improvement in the response for the latter over 5:1 was observed. Meanwhile, the yield improved gradually as the amount of catalyst increased but leveled off when the amount exceeded ca. 6 wt%. It is indicative that the methanol/acid molar ratio is a more important variable for esterification reaction than the catalyst amount; the notion is consistent with the ANOVA result (Table 4). Fig. 5b shows the correlations of catalyst amount and reaction time with methyl caprylate yield. The yield was found to increase with increasing reaction time, reaching a maximum (94.4%) at 2.0 h, then, decreased slightly thereafter. On the other hand, the yield only changed slightly with the catalyst amount. Nonetheless, the contour plot in Fig. 5e revealed that the interaction between catalyst amount and reaction time played an important role in esterification, as also indicated by the results shown in Table 4. Figs. 5c and 5f illustrate the interaction between reaction time and methanol/caprylic acid molar ratio with respect to the product yield. The yield increased significantly before the methanol/acid molar ratio reached 5:1, but remained practically unchanged beyond this ratio. A slight reduction in ester yield was observed at prolonged reaction time (> 2 h). Again, this is attributed to partial hydrolysis of the methyl caprylate product when the reaction time exceeded its maximum value (2 h). Since esterification is a reversible reaction, the hydrolysis rate of ester would increase with reaction time while the yield of methyl caprylate decreased. The effect of interaction of these two variables was also significant, revealing an ellipse mound shape (Fig. 5e), in good agreement with the ANOVA result (Table 4).

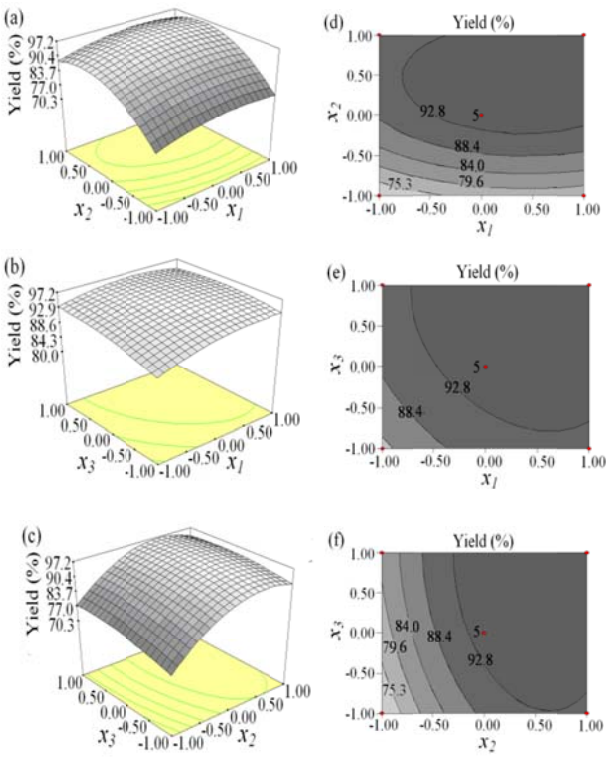

Fig. 5 (a-c) 3D response surface and (d-f) contour plots showing variations between a pair of experimental variables (Table 1) on predicted values of methyl caprylate yield while keeping other variables at a constant level of 0: (a) and (d) methanol/*n*-caprylic acid molar ratio vs catalyst amount; (b) and (e) reaction time vs catalyst amount; (c) and (f) reaction time vs methanol/*n*-caprylic acid molar ratio.

Optimized responses and model verification

Based on RSM results, the mathematical model predicted an optimal methyl caprylate yield of 96.16% for esterification of *n*-caprylic acid with methanol over the $[HSO_3\text{-pmim}]^+(½Zn^{2+})SO_4^{2-}$ AIL catalyst under the following process conditions: x_1 = 6.59 wt% (catalyst amount), x_2 = 6.17:1 (methanol/*n*-caprylic acid molar ratio), and x_3 = 2.26 h (reaction time) at a reaction temperature of 363 K. To confirm the validity of the model and optimal process conditions, three additional experiments were conducted in parallel at 363 K with x_1 = 7 wt%, x_2 = 6:1, x_3 = 2.0 h. Accordingly, methyl caprylate yields of 95.1, 95.5, and 95.7% were obtained, leading to an average experimental yield of 95.4%, in good agreement with the predicted value. Thus, it is conclusive that the model was reliable and that the regression equation could truly reflect influence of the three variables on the yield of esterification.

Catalyst recycling

To evaluate the reusability of such B-L AIL catalyst, cyclic experiments were conducted under the same optimal operating conditions obtained above over the $[HSO_3\text{-pmim}]^+(½Zn^{2+})SO_4^{2-}$. For each cycle, the lower layer of the reaction mixture was separated from the system after the esterification reaction, extracted with diethyl ether, and vacuum dried for 5 h at 393 K. The recovered $[HSO_3\text{-pmim}]^+(½Zn^{2+})SO_4^{2-}$ catalyst was assessed by ^{1}H NMR spectroscopy to ensure no traces of reactants or products were retained in the catalyst. It was found that the recovered AIL catalyst could be reused for at least five consecutive runs without significant loss in catalytic activity, as summarized in Table 5. The gradual decrease in product yield observed after repeated cycles is ascribed due to leaching of Zn. Additional elemental analysis by inductively coupled plasma (ICP) revealed that the concentration of Zn in the spent catalyst decreased from 9.71 wt% (fresh catalyst) to 9.45 wt% after the fifth run.

Table 5 Stability of the $[HSO_3\text{-pmim}]^+(½Zn^{2+})SO_4^{2-}$ AIL catalyst during esterification of *n*-caprylic acid with methanol over the $[HSO_3\text{-pmim}]^+(½Zn^{2+})SO_4^{2-}$ catalyst (Reaction conditions: x_1 = 7 w%, x_2 = 6:1, x_3 = 2 h, and T = 363 K)

Recycle time	Conversion (%)	Methyl caprylate yield (%)
1	95.9	95.4
2	95.6	95.1
3	95.2	94.6
4	93.8	93.2
5	93.0	92.6

Kinetic model

To establish the kinetic model for esterification of *n*-caprylic acid to methyl caprylate over the $[HSO_3\text{-pmim}]^+(½Zn^{2+})SO_4^{2-}$ B-L AIL catalyst, additional experiments were conducted with x_1 = 7 wt%, x_2 = 6:1, x_3 = 2.0 h at different temperatures. During the reaction, ca. 1 mL sample was withdrawn from the mixture for analysis at different time intervals.[44-46] The variations of instantaneous concentration of *n*-caprylic acid (C_A) versus reaction time at five different temperatures (323, 333, 343, 353, and 363 K) are shown in Fig. 6. Accordingly, the instant reaction rate (r) may be estimated by performing differentiation of the decay curve using a software package (Origin 8.5) to employ in the subsequent linear curve fitting to obtain values of k and α in Eq. (6).

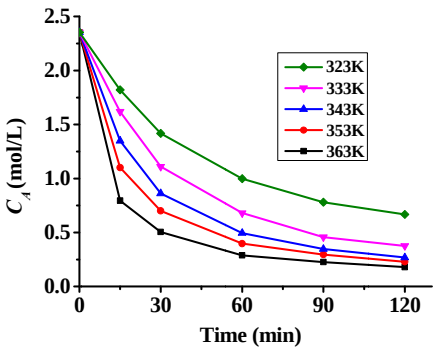

Fig. 6 Variations of instantaneous concentration of *n*-caprylic acid (C_A) with reaction time at different temperatures.

Taking the experiment conducted at 323 K as an example, the plot of ln r versus ln C_A fitted Eq. (6) well with a correlation coefficient (R) of 0.9841, as shown in Fig. 7a. Likewise, satisfactory fits were achieved for plots obtained at other temperatures. Accordingly, the k and α value so deduced from various temperatures are summarized in Table 6, from which an average reaction order α of 1.70 was derived for the esterification

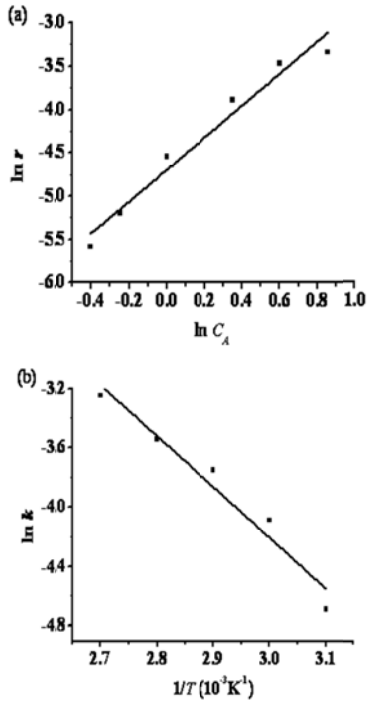

Fig. 7 Plots of (a) ln *k* vs ln C_A (at 323 K) and (b) ln *k* vs 1/T.

Table 6 List of *k* and *α* values at different temperatures during esterification of *n*-caprylic acid with methanol over the $[HSO_3\text{-pmim}]^+(½Zn^{2+})SO_4^{2-}$ catalyst

Temperature (K)	k ($mol^{-0.7}\cdot L^{0.7}\cdot min^{-1}$)	*α*
323	0.92 x 10^{-2}	1.8470
333	1.68 x 10^{-2}	1.5916
343	2.35 x 10^{-2}	1.5907
353	2.90 x 10^{-2}	1.6909
363	3.88 x 10^{-2}	1.7795

reaction. Based on Eq. (7), activation energy E_a = 33.66 kJ/mol and a pre-exponential factor k_0 = 2.86 x 10^3 may also be deduced from the slope and intercept of Arrhenius plot shown in Fig. 7b. Therefore, the kinetic equation (Eq. (5)) for esterification of *n*-caprylic acid to methyl caprylate under aforementioned optimum conditions may be expressed as:

$$r = -\frac{dC_A}{dt} = 2.86 \times 10^3 \exp(-\frac{33.66}{RT}) C_A^{1.70} \quad (9)$$

The activation energy (E_a) observed herein for the esterification of *n*- caprylic acid with methanol over the $[HSO_3\text{-pmim}]^+(½Zn^{2+})SO_4^{2-}$ AIL catalyst is lower than those obtained for esterification of palmitic acid with methanol over TPA/SnO_2 (36.33 kJ/mol)[47] and esterification of acetic acid with methanol over ResinTech SACMP-H (48.2 kJ/mol).[48] This indicates that the $[HSO_3\text{-pmim}]^+(½Zn^{2+})SO_4^{2-}$ catalyst is indeed a highly effective catalyst for esterification of *n*-caprylic acid to methyl caprylate.

Conclusions

A series of new halogen-free Brønsted-Lewis acidic ionic liquids were synthesized and exploited to catalyse esterification of *n*-caprylic acid with methanol. The $[HSO_3\text{-pmim}]^+(½Zn^{2+})SO_4^{2-}$ catalyst, which exhibited the highest catalytic activity, was employed for process optimization to obtain optimal esterification conditions at a reaction temperature of 363 K: catalyst amount of 7 wt%, methanol/*n*-caprylic acid molar ratio of 6, reaction time of 2.0 h, leading to a maximum methyl caprylate yield of 95.4%. These optimized experimental values are in good agreement with those predicted by response surface methodology based on the Box-Behnken design model. A reaction order of 1.7 and activation energy of 33.66 KJ/mol was deduced from the kinetic model developed. In addition to superior catalytic activity, the Brønsted-Lewis acidic ionic liquid catalysts report herein are also advantaged by facile recovery and recycle use without significant loss in catalytic activity. Our results indicate that the novel eco-friendly $[HSO_3\text{-pmim}]^+(½Zn^{2+})SO_4^{2-}$ catalyst is a promising substitute for conventional catalyst and of great value in chemical industry.

Acknowledgements

The supports of this work by National Natural Science Foundation of China (No. 21177110), National Natural Science Foundation of Zhejiang province, China (No. LY13B070005), and Ministry of Science and Technology, Taiwan (NSC 101-2113-M-001-020-MY3) are gratefully acknowledged.

References

1 J. Otera, *Esterification: Methods, Reactions, and Applications*, Wiley-VCH, Weinheim, 2003.
2 K. Saravanan, B. Tyagi and H. C. Bajaj, *J. Sol-Gel Sci. Technol.*, 2012, **62**, 13–17.
3 T. Parangi, B. Wani and U. Chudasama, *Appl. Catal. A: Gen.*, 2013, **467**, 430–438.
4 K. Mantri, R. Nakamura, Y. Miyata, K. Komura and Y. Sugi, *Mater. Sci. Forum*, 2007, **539–543**, 2317–2322.
5 K. Mantri, K. Komura and Y. Sugi, *Green Chem.*, 2005, **7**, 677–682.
6 Z. Zhao, Z. Li, G. Wang, W. Qiao and L. Cheng, *Progress in Chemistry* (China), 2004, **16**, 620–630.
7 S. R. Kirumakki, N. Nagaraju and K. V. R. Chary, *Appl. Catal. A: Gen.*, 2006, **299**, 185–192.
8 K. H. Chung and B. G. Park, *J. Ind. Eng. Chem.*, 2009, **15**, 388–392.
9 N. Gokulakrishnan, A. Pandurangan and P. K. Sinha, *J. Mol. Catal. A: Chem.*, 2007, **263**, 55–61.
10 D. Patel and B. Saha, *Ind. Eng. Chem. Res.*, 2012, **51**, 11965–11974.
11 D. P. C. de Barros, P. Fernanders, J. M. S. Cabral and L. P. Fonseca, *Catal. Today*, 2011, **173**, 95–102.
12 E. H. Ahmed, T. Raghavendra and D. Madamwar, *Bioresour. Technol.*, 2010, **101**, 3628–3634.
13 W. Huang, Y. M. Xia, H. Gao, Y. J. Fang, Y. Wang and Y. Fang, *J. Mol. Catal. B: Enzym.*, 2005, **35**, 113–116.
14 B. Major, I. Kelemen-Horváth, Z. Csanádi, K. Bélafi-Bakó and L. Gubicza, *Green Chem.*, 2009, **11**, 614–616.
15 J. M. Marchetti and A. F. Errazu, *Fuel*, 2008, **87**, 3477–3480.
16 R. Hagiwara and Y. Ito, *J. Fluorine Chem.*, 2000, **105**, 221–227.
17 T. Welton, *Chem. Rev.*, 1999, **99**, 2071–2083.
18 R. Juárez, R. Martín, M. Álvaro and H. García, *Appl. Catal. A: Gen.*, 2009, **369**, 133–137.
19 H. Shi, W. Zhu, H. Li, H. Liu, M. Zhang, Y. Yan and Z. Wang, *Catal. Commun.*, 2010, **11**, 588–591.
20 H. Du, Y. He, Z. Tan and X. Han, *Asian J. Chem.*, 2013, **25**, 7675–7678.
21 H. Zhu, F. Yang, J. Tang and M. He, *Green Chem.*, 2003, **5**, 38–39.

22 C. Imrie, E. R. T. Elago, C. W. McCleland and N. Williams, *Green Chem.*, 2002, **4**, 159–160.
23 C. Zhang, X. Y. Pan, M. J. Yu, L. Jin, G. Wu, *Chem. Eng. J.*, 2012, **209**, 464–468.
24 C. Chiappe, S. Rajamania and F. D'Andreab, *Green Chem.*, 2013, **15**, 137–143.
25 K. Matuszek, A. Chrobok, F. Coleman, K. R. Seddon, M. Swadźba-Kwaśny, *Green Chem.*, 2014, **16**, 3463–3471.
26 H. Wang, C. Wu, X. Bu, W. Tang, L. Li, T. Qiu, *Chem. Eng. J.*, 2014, **246**, 366–372.
27 F. Shirini, A. Yahyazadeh, K. Mohammadi, N. G. Khaligh, *C. R. Chimie*, 2014, **17**, 370–376.
28 B. Aghabarari, N. Dorostkar, M. Ghiaci, S G. Amini, E. Rahimi and M. V. Martinez-Huerta, *J. Taiwan Inst. Chem. Eng.*, 2014, **45**, 431–435.
29 Y. Yang, W. He, C. Jia, Y. Ma, X. Zhang and B. Feng, *J. Mol. Catal. A: Chem.*, 2012, **357**, 39–43.
30 D. Zhao, J. Ge, J. Zhai, J. Zhang, M. Liu and J. Li, *J. Chem. Ind. Eng.* (China), 2014, **2**,561-569.
31 S. Liu, C. Xie, S. Yu, M. Xian and F. Liu, *Chin. J. Catal.*, 2009, **30**, 401–406.
32 C. Chiappe and S. Rajamani, *Eur. J. Org. Chem.*, 2011, 5517–5539.
33 X. Liang and C. Qi, *Catal. Commun.*, 2011, **12**, 808–812.
34 A. Zheng, F. Deng and S. B. Liu, *Ann. Rep. NMR Spectrosc.*, 2014, **81**, 47–108.
35 A. Zheng, S. J. Huang, S. B. Liu and F. Deng, *Phys. Chem. Chem. Phys.*, 2011, **13**, 14889–14901.
36 A. Zheng, S. B. Liu and F. Deng, *Solid State Nucl. Magn. Reson.*, 2013, **55-56**, 12–27.
37 X. Han and L. Zhou, *Chem. Eng. J.*, 2011, **172**, 459–466.
38 X. Wu, X. Han, L. Zhou and A. Li, *Indian J. Chem.*, 2012, **51A**, 791–799.
39 A. H. M. Fauzi and N. A. S. Amin, *Energy Convers. Manage.*, 2013, **76**, 818–827.
40 X. Han, Y. He, C. T. Hung, L. L. Liu, S. J. Huang, and S. B. Liu, *Chem. Eng. Sci.*, 2013, **104**, 64–72.
41 Y. Leng, P. Jiang and J. Wang, *Catal. Commun.*, 2012, **25**, 41–44.
42 X. Tong, N. Tian, W. Zhu, Q. Wu, F. Cao and W. Yan, *J. Alloys Compd.*, 2012, **544**, 37–41.
43 Y. Chu, Z. Yu, A. Zheng, H. Fang, H. Zhang, S. J. Huang, S. B. Liu and F. Deng, *J. Phys. Chem. C*, 2011, **115**, 7660–7667.
44 T. Garcia, A. Coteron, M. Martinez and J. Aracil, *Chem. Eng. Sci.*, 2000, **55**, 1411–1423.
45 D. J. Tao, Y. T. Wu, Z. Zhou, J. Geng, X. B. Hu and Z. B. Zhang, *Ind. Eng. Chem. Res.*, 2011, **50**, 1989–1996.
46 A. Talebian-Kiakalaieh, N. A. S. Amin, A. Zarei and I. Noshadi, *Appl. Energy*, 2013, **102**, 283–292.
47 K. Srilatha, C. R. Kumar, B. L. A. P. Devi, R. B. N. Prasad, P. S. S. Prasad, and N. Lingaiah, *Catal. Sci. Technol.*, 2011, **1**, 662–668.
48 E. Sert and F. S. Atalay, *Prog. React. Kinet. Mec.*, 2011, **36**, 239–251.